

## Supplementary material

The implications of the effective  $B_s^0 \rightarrow K^+K^-$  lifetime measurement is the overall reduction in the uncertainty to 0.017 ps compared with previous measurements, this can be seen in Fig. 3.

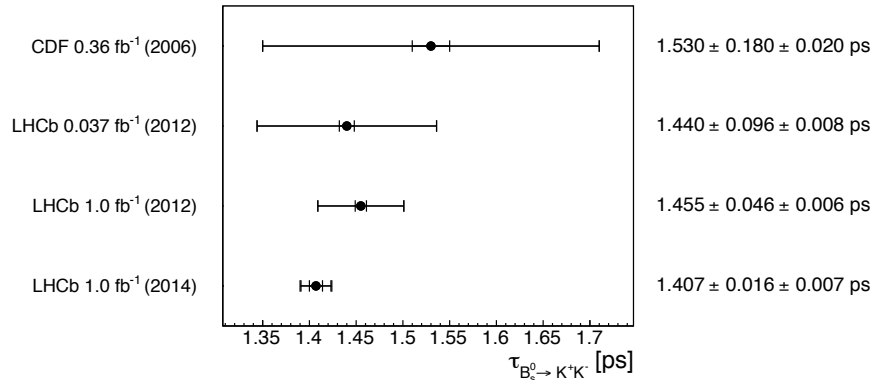


Figure 3: Evolution of the effective  $B_s^0 \rightarrow K^+K^-$  lifetime through all previous measurements. The statistical uncertainties are represented by the inner error bars, with the outer error bars representing the total uncertainty of the measurement.

Constraints on the decay width difference  $\Delta\Gamma_s$  and the  $B_s^0-\bar{B}_s^0$  mixing phase  $\phi_s$  are shown in Fig. 4 together with the SM predictions.

A comparison of the  $B^0$  lifetime measured in this analysis, compared to previous measurements, is given in Fig. 5.

Previously measured flavour specific lifetimes of the  $B_s^0$  meson, compared with the lifetime measured by this analysis, are provided in Fig. 6.

The *sPlots* [29] of the individual signal channel lifetimes are given in Figs. 7 8 and 9.

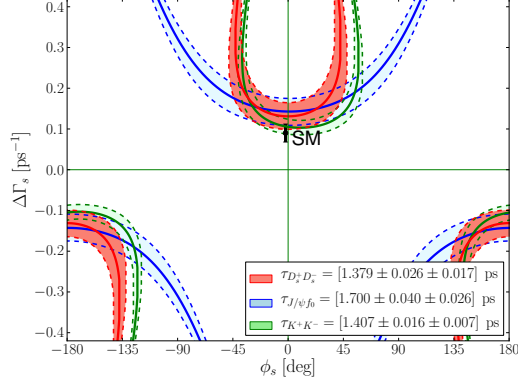


Figure 4: Constraints on  $\phi_s$  and  $\Delta\Gamma_s$ , which are the mixing phase between the  $B_s^0$  and  $\bar{B}_s^0$  and decay width difference respectively, using three recent effective lifetime measurements from LHCb. Figure made using the formalism described in Ref. [12].

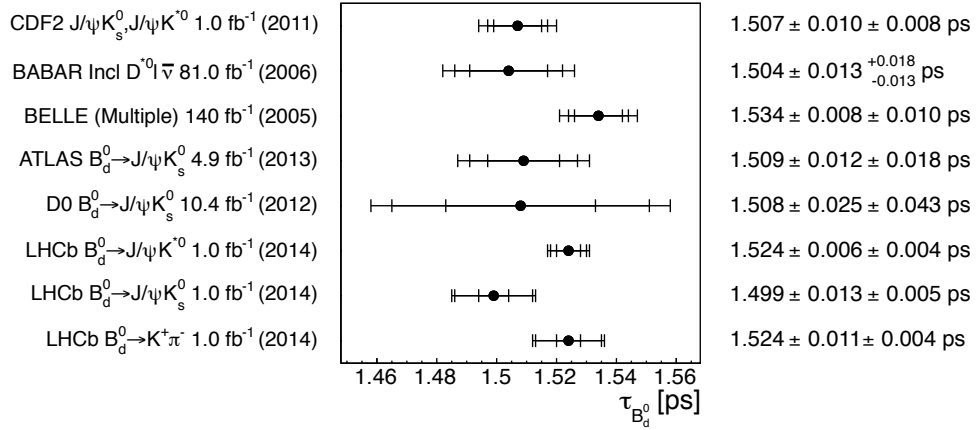


Figure 5: Evolution of the  $B^0$  lifetime through selected previous measurements. Systematic errors are represented by the inner error bars, with the second largest error bars representing the statistical uncertainty and the largest error bars representing the total uncertainty of the measurement.

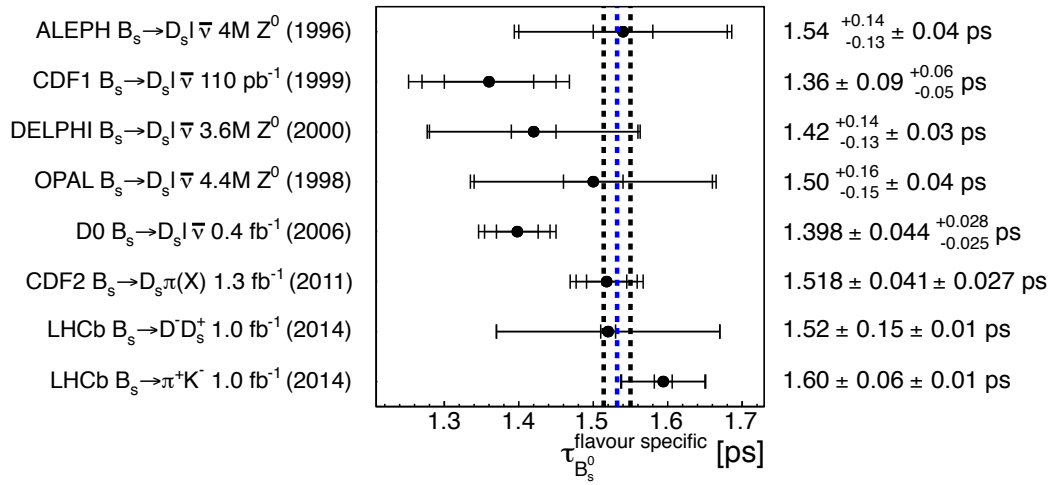


Figure 6: Evolution of the flavour specific  $B_s^0$  lifetime through all previous measurements. Systematic errors are represented by the inner error bars, with the second largest error bars representing the statistical uncertainty and the largest error bars representing the total uncertainty of the measurement. The blue vertical dotted line represents the flavour specific lifetime predicted using Eq. 2, with the measured values of  $\Delta\Gamma_s$  and  $\Gamma_s$  taken from  $B_s^0 \rightarrow J/\psi \phi$  in Ref. [13]. The black vertical dotted lines represent the uncertainties predicted from these measurements.

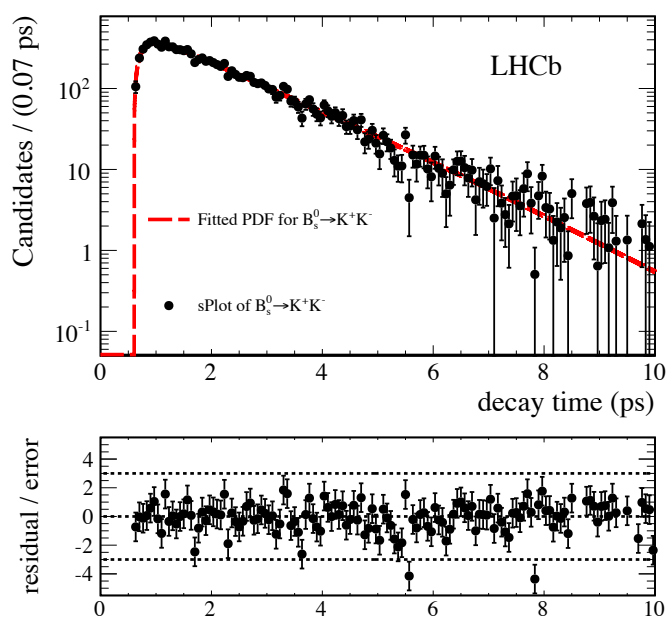


Figure 7: The dashed line shows the fitted decay time PDF for the  $B_s^0 \rightarrow K^+ K^-$  signal multiplied by the average acceptance function determined from the per-event acceptance functions and the *sWeights*. The data points show an *sPlot* of the  $B_s^0 \rightarrow K^+ K^-$  decay time.

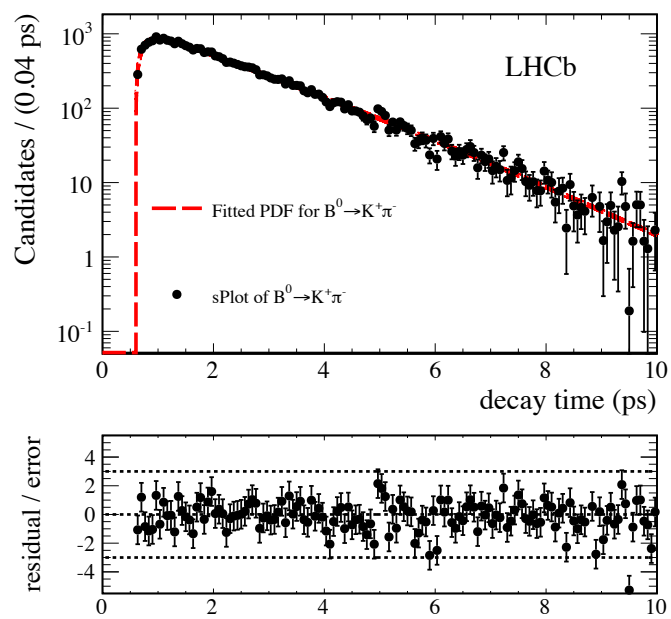


Figure 8: The dashed line shows the fitted decay time PDF for the  $B^0 \rightarrow K^+ \pi^-$  signal multiplied by the average acceptance function determined from the per-event acceptance functions and the *sWeights*. The data points show an *sPlot* of the  $B^0 \rightarrow K^+ \pi^-$  decay time.

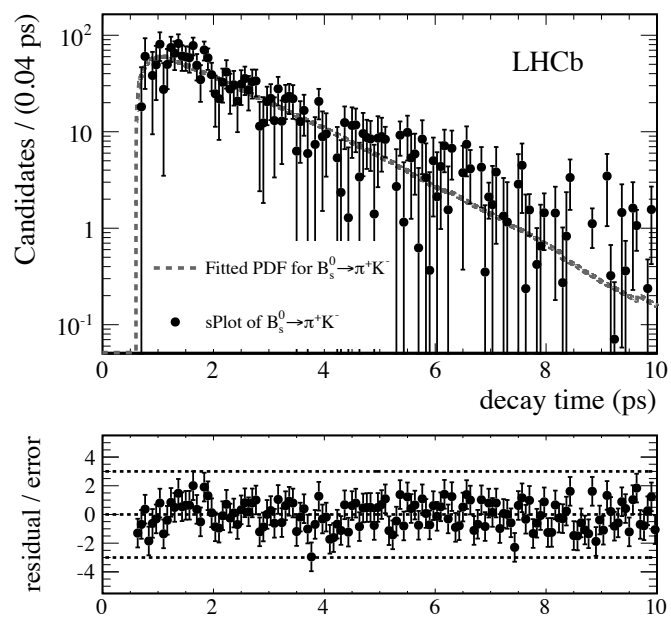


Figure 9: The dashed line shows the fitted decay time PDF for the  $B_s^0 \rightarrow \pi^+ K^-$  signal multiplied by the average acceptance function determined from the per-event acceptance functions and the  $sWeights$ . The data points show an  $sPlot$  of the  $B_s^0 \rightarrow \pi^+ K^-$  decay time.